NSS

Neutrosophic Sets and Systems, Vol. 86, 2025

University of New Mexico

Differential Quadri-Partitioned Neutrosophic Interval-Valued Polynomial Attention-Based Deep CNN For Brain Tumor Detection

Panimalar A[1], Aarthi D[2], Santhosh Kumar S[3,*]and Sanjayprabu S[4]

[1]KGiSL Institute of Technology, Coimbatore; panimalar81@gmail.com

[2]Sri Ramakrishna Mission Vidyalaya College of Arts and Science, Coimbatore; aarthi.pkm16@gmail.com

[3]Sri Ramakrishna Mission Vidyalaya College of Arts and Science, Coimbatore; fuzzysansrmvcas@gmail.com

[4]Rathinam College of Liberal Arts and Science @ TIPS Global, Coimbatore; sanjayprabu.maths@gmail.com

[*]Correspondence: fuzzysansrmvcas@gmail.com;

Abstract. Brain tumor image classification is a vital part of the medical image area. Early treatment diagnosis of brain tumors is challenging through the Magnetic Resonance Imaging (MRI) in clinical neuroradiology. Brain tumor detection is a development of vital significance where Convolutional Neural Networks (CNN) find application. However, the accuracy and time required to detect brain tumors is a large challenge. To address the issue, the proposed Differential Quadri-partitioned Neutrosophic Interval-valued Polynomial Attention-based Deep CNN (DQNI-PADCNN) is introduced for brain tumor detection. Initially, the region of interest (RoI) detection is performed by using Differential Quadripartitioned Neutrosophic Sets. After RoI detected brain tumor images, classification is carried out via Interval-valued Quadripartitioned Neutrosophic Polynomial Attention-based Deep Convolutional Neural Network. The designed model includes convolutional layers, pooling layers, and fully connected layers. In the convolutional layer, feature maps consider RoI brain tumor images. Feature maps are sampled down and offered as input to the pooling layers. In this layer, the ELU function is estimated. Finally, the brain tumor detection result is obtained in the fully connected layer with higher accuracy and less time. Experimental evaluation is carried out by using the brain tumor dataset with different factors, such as the PSNR, the brain tumor detection accuracy, the brain tumor detection time, sensitivity, and specificity. The results confirm that the proposed technique achieves higher accuracy of the PSNR and disease detection with a minimum of time and space complexities than the conventional classification methods.

Keywords: Brain Tumor; Magnetic Resonance Imaging; Differential Quadri-partitioned Neutrosophic Set; Region of Interest detection;. Polynomial Attention; Interval-valued Deep Convolutional Neural Network.

1. Introduction

The Brain tumors are one of the most regular sources of human death. Therefore, an early and precise diagnosis is analytical for an efficient therapeutic process. In clinical neuroradiology, preliminary treatment diagnosis of brain tumors utilizing Magnetic Resonance Imaging (MRI) is demanding. Today, the association of Information Technology (IT) and digital healthcare techniques in the medical domain aids physicians in achieving better quality health services for the diseased.

A novel deep learning technique for detecting brain tumors was proposed in [1]. Here, initially, a compound filter was applied as a preprocessing system integrating three types of filters, namely, Gaussian, mean and median filters. Following the preprocessed output, image segmentation was performed employing threshold and histogram techniques. Next, pertinent features were extracted using Grey Level Co-occurrence Matrix (GLCM). Optimal feature selection was then made via optimized convolution neural network (CNN) using whale and grey wolf optimization and finally, the CNN classifier was applied for accurate brain tumor detection. The method was proved to be efficient in terms of accuracy, precision, and recall. Nevertheless, these tests had certain disadvantages that in turn resulted in detection delays.

A convolutional Neural Network (CNN)-based brain tumor diagnosis method was proposed in [2] by employing EfficientNetv2s architecture. Here, introducing an optimization technique using the Ranger function and a considerable amount of preprocessing not only resulted in accuracy improvement but also minimized the delay factor considerably.

A survey was conducted in [3] on brain tumor detection via MRI to assist the researchers in performing brain tumor analysis. Nevertheless, manual brain detection is considered a time consuming and laborious process that can result in even erroneous analysis. The application of computer-aided techniques assists in addressing these limitations.

In [4], a deep convolutional neural network (CNN) EfficientNet-B0 was fine-tuned with the purpose of significantly classifying the detecting brain tumor images. The conventional machine learning techniques utilized handcrafted feature for performing classification, whereas deep learning techniques without handcrafted feature extraction achieved precision classification results. Two deep learning techniques were designed in [5] for identifying normal and multiclass brain tumors with which classification accuracy was ensured. As far as clinical practice is concerned, distinct radiographic image modalities are seen to be utilized in different types of brain tumors, their size, and location. In [6], an automatic classification, localization, and segmentation method from T1W-CE Magnetic Resonance Image (MRI) datasets were designed. Also, by using a pre-trained model considerable amount of accuracy was ensured. Yet another accurate and automatic brain tumor detection method employing CNN-based deep learning was presented in [7]. Nevertheless, a precise integration of convolution and attention

to enhance brain tumor segmentation is still considered an interesting issue to be addressed. UNet architecture with the inclusion of attention and replacement of processing block with dual convolution sequences referred to as the Multipath Residual Attention Block (MRAB) was proposed in [8]. Despite several important endeavors and inspiring results, accuracy and classification continue to be demanding issues. An assessment matrix employing specific systems and dataset types to elucidate the brain tumor morphology employing machine learning, deep learning, and transfer learning was investigated in [9]. In [10], automatic brain tumor detection using ensemble deep learning architectures like, Inception V3, and Mobile Net were presented. This type of ensemble technique not only improved the accuracy rate but also reduced error significantly. The inception of the analysis of images in a quantitative manner has given rise to fields like radiomics for accurate clinical prediction. Among them, the growing area of interest is brain tumor analysis.

1.1. *Research Gap*

Detection and Classification of brain tumors is a significant part of image processing. MRI helps the radiologist discover the tumor region. Several conventional methods were developed for detecting brain tumors. But, the time was higher to detect brain tumors. Early diagnosis of a brain tumor is vital for classification. However, the accurate brain detection rate was insufficient. Also, the brain tumor diagnosis approaches failed to enhance image quality. The motivation of this research is to conduct extensive experimentation using deep convolutional neural networks to automate the process of brain tumor classification and detection.

1.2. *Novelty and Contributions of the Paper*

This paper presents a brain tumor detection method in which Differential Quadri-partitioned Neutrosophic-based Region of Interest detection algorithms are used along with Interval-value and Polynomial Attention-based Deep Convolutional Neural Network. The contributions of the work include the following:

- To accurately detect brain tumor detection, the proposed DQNI-PADCNN is introduced
- To improve the region of interest detection, Novel Differential Quadri-partitioned Neutrosophic is introduced in the proposed DQNI-PADCNN for accurate brain tumor diagnosis. In this way, sensitivity and specificity are improved.
- To classify the brain tumor images into glioma, meningioma, no tumor, and pituitary, Deep Convolutional Neural Network is applied with the innovation of Interval-valued and Polynomial Attention. It comprises pooling layers, convolutional layers, and fully connected layers. Quadri-partitioned convolution layer is employed for every RoI brain

tumor image. Also, the Polynomial Attention Coefficient function is measured in the convolution layer. Then, the ELU function is applied in the pooling layer. Lastly, the output generated from the fully connected layers for better accuracy and timely learning procedure of the brain tumor diagnosis.

- Extensive experimental evaluation of the DQNI-PADCNN method against deep learning technique and CNN-based brain tumor classification to demonstrate the superior predictive performance of the proposed method by analyzing performance metrics like PSNR, specificity, brain tumor detection accuracy, and brain tumor detection time.

1.3. *Organization of the work*

In the general structure of this work, Section 2 reviews related works on brain tumor detection employing, machine learning and deep learning techniques. Following this a detailed description of the proposed method with some considerations on the RoI detection tasks and classification for brain tumor detection with the aid of an algorithm is presented in Section 3. In Section 4, the experimental setup along with the dataset description is provided. Section 5 discusses in terms of both the quality and quantitative analysis with the aid of graphs and tables via case study. Finally, section 6 introduces the conclusions.

2. **Related Works**

The role of CNN for accurate and precise brain tumor segmentation was investigated in [11]. Yet another method employing CNN with regularization, fine tuning of momentum, and introduction of loss functions was investigated in [12]. The classification of brain tumors is yet considered a challenging issue in the medical image processing domain. A hybrid method employing Neutrosophy and Convolutional Neural Networks called (NS-CNN) was presented in [13]. The method was designed with the objective of improving the accuracy and reducing errors involved in classifying tumor region areas as benign and malignant. A survey employing deep learning techniques for multi-grade brain tumor classification was investigated in [14]. Yet another three-dimensional CNN was designed in [15] focusing on the classification accuracy aspect. In [16], a novel correlation mechanism employing a learning technique that integrated CNN with a traditional framework was proposed. The support neural network assisted CNN in identifying the pertinent filers for both pooling and convolution. With this, the main neural classifier convergence speed was proven to be faster therefore ensuring higher efficiency. The prevailing method was however found to be laborious and time-consuming susceptible to human errors. These drawbacks show how mandatory it is to perform a fully automatic multi-classification method for brain tumors based on deep learning. In [17], brain tumor multiclassification for early diagnosis employing CNN was presented to focus on the

accuracy and timeliness aspects. Neutosophic logic which consists of logic, set theory, and probability/statistics, can depict the imprecision arising due to tumor detection. In [18], a comprehensive introduction regarding image processing with the inclusion of uncertainty was stated. Following this, the neutrosophic sets for image processing were also expressed. Yet another fuzzy CNN employing neutrosophic logic was designed in [19] with the focus laid on accurate tumor detection. An automatic classification employing a complex neural network was designed in [20]. In [21] Quadri-Partitioned neutrosophic set properties and definitions were discussed. Also, the algebraic properties for morphology in the Quadri partitioned set were defined. Secant span was employed in [24] for handling medical diagnosis issues with maximum accuracy. But, the time was not minimized. DNA sequence-matching algorithm was introduced in [23] for determining similarity. However, if failed to consider the specificity. Although numerous valuable studies on brain tumor diagnosis using several DL algorithms have been proposed have is room for improvement in overall performance. In this work, a method called, Differential Quadri-partitioned Neutrosophic Interval-valued Polynomial Attention-based Deep CNN (DQNI-PADCNN) is proposed focusing on the aspects of PSNR, specificity, brain tumor detection accuracy, and brain tumor detection time.

3. Differential Quadri-partitioned Neutrosophic Interval-valued Polynomial Attention-based Deep Convolutional Neural Network (DQNI-PADCNN)

Brain tumor is contemplated as a grave disease, wherein brain MRI image plays a significant part. The impact of brain tumor detection comprises early detection, improved image quality and accuracy, tumor classification and lesser detection time has significant improvements in diagnosis. Accuracy in brain tumor diagnosis assists in accurately detecting the regions contrived by the tumor, and furthermore, reduces the mortality rate. As a result, hidden pattern detection is mandatory for achieving enhanced diagnosis and boosting image quality. Nevertheless, it becomes a crucial point at issue in obtaining precise diagnosis taking into consideration distinct cases of lesion. To address these aspects faced by traditional methods, in this work, Differential Quadri-partitioned Neutrosophic Interval-valued Polynomial Attention-based Deep CNN (DQNI-PADCNN) is proposed. Differential Quadri-partitioned Neutrosophic is used to find ROI with higher PSNR. Deep CNNs are employed to find brain tumors at earlier stages due to their higher sensitivity for timely treatment interventions. Deep CNNs are used to obtain higher accuracy and less time in brain tumor detection. Deep CNNs are developed for categorizing dissimilar types of brain tumors for treatment planning and prognosis. An elaborate description of DQNI-PADCNN is provided in the following sections.

3.1. *Differential Quadri-partitioned Neutrosophic-based Region of Interest detection*

In this work, an extensively organized method is designed to classify MR brain image, to assist the clinician to stick with the correct decision. Nevertheless, making a precise decision is not possible at a first sight. Here, biased feature image representation (i.e., customized region of interest) must be seized from brain MRI, with the intention of getting enhanced feature representation. The method proposes a novel classification model where customized region of interest is identified by the Quadri-partitioned Neutrosophic Set model. To employ the Quadri-partitioned Neutrosophic Set (QNS) designing for detecting region of interest (RoI) towards brain tumor detection, the input brain image must be converted to a QNS field. In our work, the region of interest is detected by employing Differential Quadri-partitioned Neutrosophic model. Figure 1 shows the structure of Differential Quadri-partitioned Neutrosophic-based Region of Interest detection model.

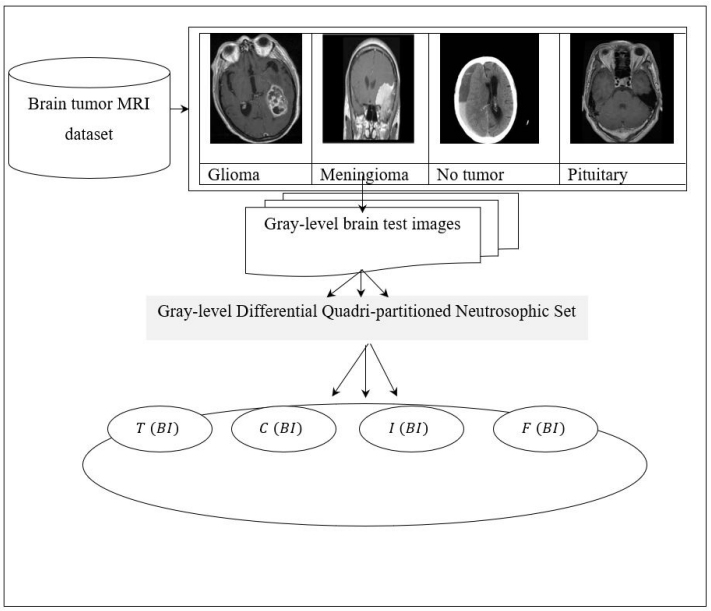

FIGURE 1. Structure of Differential Quadri-Partitioned Neutrosophic-based Region of Interest detection model.

With the hypothesis that the QNS-based image processing is expanded into four levels, namely, degrees of truth 'T', degrees of contradiction 'C', degrees of ignorance 'I', and degrees of falsehood 'F' subsets, and a brain test image 'BI' with length 'len' and width 'wid' respectively, the QNS-based brain test image is visualized by the format as given below:

$$BI = \{\langle \mathrm{BI}, T_{\mathrm{out}}(\mathrm{BI}), C_{\mathrm{out}}(\mathrm{BI}), I_{\mathrm{out}}(\mathrm{BI}), F_{\mathrm{out}}(\mathrm{BI})\rangle\} \quad (1)$$

From the above format (1), $T_{\text{out}}(\text{BI}), C_{\text{out}}(\text{BI}), I_{\text{out}}(\text{BI}), F_{\text{out}}(\text{BI})$ represent the true membership subset, contradiction membership subset, ignorance membership subset, and false membership subset with their subsequent length and width respectively [23, 24].

$$T(\text{len}, \text{wid}) = \frac{g'(\text{len}, \text{wid}) - g_{\min}}{g'_{\max} - g'_{\min}} \tag{2}$$

$$g'(\text{len}, \text{wid}) = \frac{1}{W \cdot W} \sum_{m=\text{len}-\frac{w}{2}}^{\text{len}+\frac{w}{2}} \sum_{n=\text{wid}-\frac{w}{2}}^{\text{wid}+\frac{w}{2}} g(\text{len}, \text{wid}) \tag{3}$$

$$F(\text{len}, \text{wid}) = 1 - T(\text{len}, \text{wid}) = \frac{g'_{\max} - g'(\text{len}, \text{wid})}{g'_{\max} - g'_{\min}} \tag{4}$$

$$I(\text{len}, \text{wid}) = \frac{\delta' - \delta'_{\min}}{\delta'_{\max} - \delta'_{\min}}, \quad \delta_{\max} = \max \delta(\text{len}, \text{wid}), \quad \delta_{\min} = \min \delta(\text{len}, \text{wid}) \tag{5}$$

$$\delta(\text{len}, \text{wid}) = |g(\text{len}, \text{wid}) - g'(\text{len}, \text{wid})| \tag{6}$$

$$C(\text{len}, \text{wid}) = 1 - I(\text{len}, \text{wid}) \tag{7}$$

Also, from the above equations 2, 3, 4, 5, 6, and 7, the truth membership, false membership, contradiction membership, and ignorance membership results for the corresponding brain test image BI with len and wid are arrived at for further processing. Moreover, $g'_{\max}$ and $g'_{\min}$ represent the maximum and minimum values of the gray-level QNS brain test images, while $g(\text{len}, \text{wid})$ represents the length and width of the gray-level QNS brain test image. The focal advantage of the above formulations remains in controlling truth, false, ignorance, and contradiction subsets between the ranges 0 and 1. Integrating the hitherto acquired quadripartitioned neutrosophic components T, F, C, and I can contribute to acquiring absolute information about inherited variability in the problem space (i.e., glioma brain tumor detection).

3.1.1. *Definition - Differential Quadri -partitioned Neutrosophic Entropy Set*

Then, the differential entropy of corresponding Quadri-partitioned Neutrosophic set 'QNS' as defined in [25, 26] is mathematically stated as given below.

$$\begin{aligned} \mathit{DiffEnt}(NS) = \int \Bigg(1 - \frac{1}{3} \sum_{(\text{len},\text{wid}) \in G} (& T(\text{len}, \text{wid}) + F(\text{len}, \text{wid}) \\ & + C(\text{len}, \text{wid}) + I(\text{len}, \text{wid}) \cdot \mathit{Ent}_1 \cdot \mathit{Ent}_2 \cdot \mathit{Ent}_3) \cdot \mathit{Ent}_4 \end{aligned} \tag{8}$$

$$\mathit{DiffEnt}_1 = \int \left[T(\text{len}, \text{wid}) - T'(\text{len}, \text{wid}) \right], \quad \textit{where} \quad T'(\text{len}, \text{wid}) = F(\text{len}, \text{wid}) \tag{9}$$

$$\mathit{DiffEnt}_2 = \int \left[F(\text{len}, \text{wid}) - F'(\text{len}, \text{wid}) \right], \quad \textit{where} \quad F'(\text{len}, \text{wid}) = T(\text{len}, \text{wid}) \tag{10}$$

$$\mathit{DiffEnt}_3 = \int \left[C(\text{len}, \text{wid}) - C'(\text{len}, \text{wid}) \right], \quad \textit{where} \quad C'(\text{len}, \text{wid}) = I(\text{len}, \text{wid}) \tag{11}$$

$$\mathit{DiffEnt}_4 = \int \left[I(\text{len}, \text{wid}) - I'(\text{len}, \text{wid}) \right], \quad \textit{where} \quad I'(\text{len}, \text{wid}) = 1 - C(\text{len}, \text{wid}) \tag{12}$$

With the above formulates as input, let us consider the representation of two QNS brain test images given by BI_i and BI_j. These QNS brain test images possess L degrees of grayness and $G(\text{len}, \text{wid})$ denotes the magnitude of the brain test image at the specific locality (len, wid) where (len, wid) differs between 0 and 255. The QNS brain test images along with the degree of magnitude for BI_i are then written as given below.

$$BI_i = \begin{bmatrix} G(1,1) & G(1,2) & \cdots & G(1,\text{wid}) \\ G(2,1) & G(2,2) & \cdots & G(2,\text{wid}) \\ \vdots & \vdots & \ddots & \vdots \\ G(\text{len},1) & G(\text{len},2) & \cdots & G(\text{len},\text{wid}) \end{bmatrix} \tag{13}$$

From the above formulate 13, 'len' and 'wid' denote the length and width of the QNS brain test image BI_i and $G(\text{len}, \text{wid}) \in BI_i$. In a similar manner, QNS brain test images along with the degree of magnitude for BI_j are formed. Following which, each gray-level QNS brain test image element $G(\text{len}, \text{wid})$ of the brain test images is characterized individually in the NS matrix representation as given below.

$$BI(QNS) = \begin{bmatrix} \langle T(1,1)\ F(1,1)\ C(1,1)\ I(1,1)\rangle & \langle T(1,2)\ F(1,2)\ C(1,2)\ I(1,2)\rangle & \cdots & \langle T(1,\text{wid})\ F(1,\text{wid})\ C(1,\text{wid})\ I(1,\text{wid})\rangle \\ \langle T(2,1)\ F(2,1)\ C(2,1)\ I(2,1)\rangle & \langle T(2,2)\ F(2,2)\ C(2,2)\ I(2,2)\rangle & \cdots & \langle T(2,\text{wid})\ F(2,\text{wid})\ C(2,\text{wid})\ I(2,\text{wid})\rangle \\ \vdots & \vdots & \ddots & \vdots \\ \langle T(\text{len},1)F(\text{len},1)C(\text{len},1)I(\text{len},1)\rangle & \langle T(\text{len},2)F(\text{len},2)C(\text{len},2)I(\text{len},2)\rangle & \cdots & \langle T(\text{len},\text{wid})F(\text{len},\text{wid})C(\text{len},\text{wid})I(\text{len},\text{wid})\rangle \end{bmatrix} \tag{14}$$

Finally, differential entropy of QNS brain test images is modeled individually in *'QNS'* matrix with which the region of interest for brain tumor detection is represented as given below.

$$RoI = \begin{bmatrix} DiffEnt(QNS(1,\ 1)) & DiffEnt(QNS(1,\ 2)) & \cdots & DiffEnt(QNS(1,\ wid)) \\ DiffEnt(QNS(2,\ 1)) & DiffEnt(QNS(2,\ 2)) & \cdots & DiffEnt(QNS(2,\ wid)) \\ \vdots & \vdots & \ddots & \vdots \\ DiffEnt(QNS(len,\ 1)) & DiffEnt(QNS(len,\ 2)) & \cdots & DiffEnt(QNS(len,\ wid)) \end{bmatrix} \tag{15}$$

From the above formulated results differential Quadri-partitioned Neutrosophic regions of interest are obtained for corresponding brain test images. The flowchart of Differential Quadri-partitioned Neutrosophic-based Region of Interest detection is described in Figure 2.

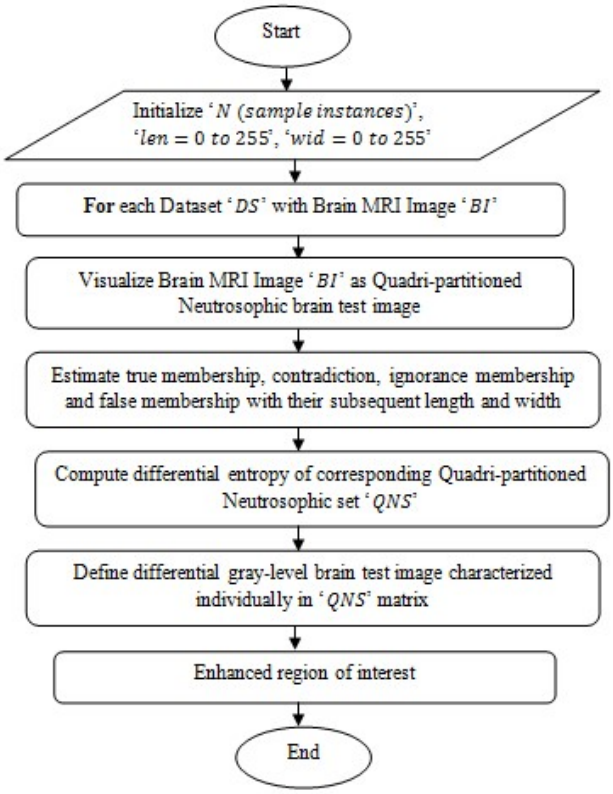

FIGURE 2. Flowchart of Differential Quadri-partitioned Neutrosophic-based Region of Interest Detection.

The pseudo code representation of Differential Quadri-partitioned Neutrosophic-based Region of Interest detection is given below. As given in the below algorithm to detect the region of interest with improved PSNR, Differential Quadri-partitioned Neutrosophic Set is applied to the raw brain tumor MRI dataset. By applying the Differential Quadri-partitioned Neutrosophic Set for detecting RoI, all four measures, i.e., truth, false, contradiction and indeterminate results are obtained without affecting others in the decision-making process. With this by addressing the uncertainty involved in raw brain tumor MRI dataset and dealing the concept of indeterminacy in an efficient manner, the Peak Signal-to-Noise-Ratio (PSNR) is said to be improved, therefore corroborating the objective.

Input	Dataset 'DS', Brain MRI Image 'BI = $\{ BI_1, BI_2, \ldots, BI_N\}'$
Output	Robust and specificity improved region of interest detection
Steps	
1	Initialize 'N (sample instances)', 'len = 0 to 255', 'wid = 0 to 255'
2	Begin
3	For each Dataset 'DS' with Brain MRI Image 'BI'
4	Visualize Brain MRI Image 'BI' as Quadri-partitioned Neutrosophic brain test image as given in (1)
5	Obtain true membership subset, contradiction membership subset, ignorance membership subset and false membership subset with their subsequent length and width as given in (2), (3), (4), (5), (6) and (7)
6	Evaluate differential entropy of corresponding Quadri-partitioned Neutrosophic set 'QNS' as given in (8), (9), (10), (11) and (12)
7	Formulate differential gray-level brain test image characterized individually in 'QNS' matrix as given in (13) and (14)
8	Obtain region of interest as given in (15)
9	Return region of interest 'RoI'
10	End for
11	End

Algorithm 1. Differential Quadri-partitioned Neutrosophic-based Region of Interest detection

3.2. *Interval-valued Quadri-partitioned Neutrosophic Polynomial Attention-based Deep Convolutional Neural Network*

With the obtained RoI by addressing the uncertainty involved in raw brain tumor MRI dataset employing Differential Quadri-partitioned Neutrosophic-based Region of Interest detection, in this section, Interval-valued Quadri-partitioned Polynomial Attention-based DCNN model is designed. Figure 3 shows the structure of Interval-valued Quadri-partitioned Neutrosophic Polynomial Attention-based DCNN model.

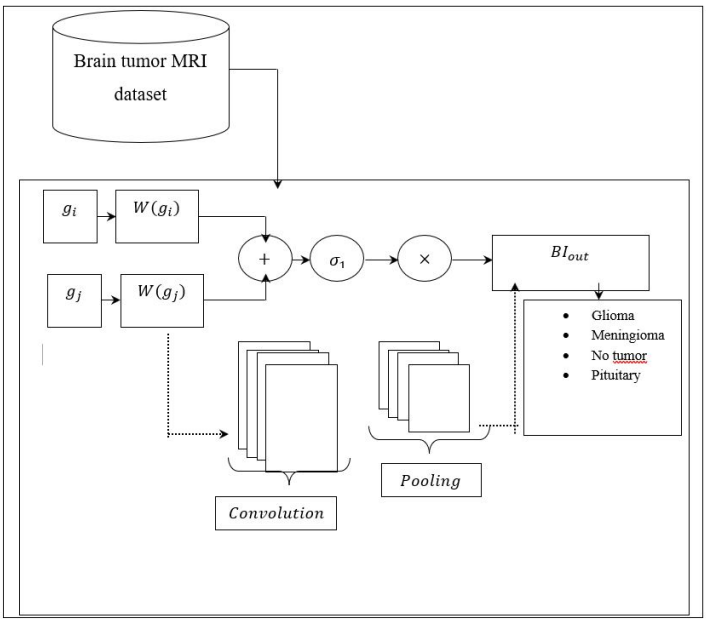

FIGURE 3. Structure of Interval-valued Quadri-partitioned Neutrosophic Polynomial Attention-based CNN model.

The structural design of the Interval-valued Quadri-partitioned Neutrosophic Polynomial Attention-based CNN model is portrayed in this section using figure. The Interval-valued Quadri-partitioned Neutrosophic Polynomial Attention-based CNN model consists of pooling layers, convolutional layers, and fully connected layers. The convolutional layer establishes the feature maps considering the RoI brain tumor images and the feature maps are further sampled down and provided as input to the pooling layers, that forms the second layer in Interval-valued Quadri-partitioned Neutrosophic Polynomial Attention-DCNN model. Finally, the fully connected layer result in the classification process. Here, the interval-valued represents the modeling of classifier results in the fully connected layer where according to the interval, four distinct classes of brain tumor detected results are obtained.

3.2.1. *Definition - Convolution layer magnitude representation*

The input to the convolution layer is RoI brain tumor images generated as the result of Differential Neutrosophic process and the magnitude of the convolution layers is given below.

$$CL = \{CL_1, CL_2, \ldots, CL_l, \ldots, CL_k\} \tag{16}$$

From the above formulates (16), 'k' refers to the number of convolution layers [26,27] and 'CL_l' indicate the l^{th} convolution layer in Polynomial Attention-DCNN model. With the above derived magnitude for each RoI brain tumor images at the convolution layer, the portions

found at 'p, q' acquire the output. Then, the Quadri-partitioned Neutrosophic convolution layer for each RoI brain tumor image is modeled as given below.

$$(CL_v^h)_{(p,q)}(T[RoI]) = (TBI_v^h)_{(p,q)} + \sum_{p=1}^{\text{size}(FM)} \sum_{i=1}^{m} \sum_{j=1}^{n} \left(FM_{\text{train},p}^i\right)_{(i,j)} \cdot (CL_v^{(h-1)})_{(p+i,q+j)} \quad (17)$$

$$(CL_v^h)_{(p,q)}(F[RoI]) = (FBI_v^h)_{(p,q)} + \sum_{p=1}^{\text{size}(FM)} \sum_{i=1}^{m} \sum_{j=1}^{n} \left(FM_{\text{train},p}^i\right)_{(i,j)} \cdot (CL_v^{(h-1)})_{(p+i,q+j)} \quad (18)$$

$$(CL_v^h)_{(p,q)}(C[RoI]) = (CBI_v^h)_{(p,q)} + \sum_{p=1}^{\text{size}(FM)} \sum_{i=1}^{m} \sum_{j=1}^{n} \left(FM_{\text{train},p}^i\right)_{(i,j)} \cdot (CL_v^{(h-1)})_{(p+i,q+j)} \quad (19)$$

$$(CL_v^h)_{(p,q)}(I[RoI]) = (IBI_v^h)_{(p,q)} + \sum_{p=1}^{\text{size}(FM)} \sum_{i=1}^{m} \sum_{j=1}^{n} \left(FM_{\text{train},p}^i\right)_{(i,j)} \cdot (CL_v^{(h-1)})_{(p+i,q+j)} \quad (20)$$

From the above equations (17), (18), (19), and (20), '*' refers to the convolution operator with $(CL_v^{(h-1)})$ referring to the brain pattern extraction obtained from adjoining convolution layers, $FM_{\text{train},p}^i$ representing the feature map for convolution to be trained using the Polynomial Attention Coefficient function concerning truth membership, false membership, contradiction membership, and ignorance membership subsets, respectively. Due to that, brain tumor MRI images are classified into four classes (i.e., glioma, meningioma, no tumor, and pituitary). We employ Interval-valued in addition to the polynomial attention coefficient to focus on a subset of target regions. The polynomial attention coefficient is mathematically stated as given below.

$$\alpha_i = \sigma_1 \left[W_G^T G_i + W_G^T G_j + b_i\right] + b_j, \quad \text{where } G_i, G_j \in BI \quad (21)$$

From the above formulation (21), 'σ_1' is selected as the Exponential Linear Unit (ELU) activation function in contrast to ReLU [1], which produces classified results based on the interval and thus assists in enhancing classification accuracy in an optimal training time.

3.2.2. *Definition - Rectified Linear Unit activation function*

The ReLU activation function for correction layer transforms all negative values received as inputs by zeros by acting as activation function as given below.

$$\text{ReLU}(G) = \max(0, G) \quad (22)$$

Then, the Quadri-partitioned Neutrosophic ReLU activation function is mathematically stated as given below.

$$\text{ReLU}\left(G\left[(\mathbf{CL}_v^h)_{(p,q)}(T[\text{RoI}])\right]\right) = \max\left(0, G\left[(\mathbf{CL}_v^h)_{(p,q)}(T[\text{RoI}])\right]\right) \quad (23)$$

$$\text{ReLU}\left(G\left[(\mathbf{CL}_v^h)_{(p,q)}(F[\text{RoI}])\right]\right) = \max\left(0, G\left[(\mathbf{CL}_v^h)_{(p,q)}(F[\text{RoI}])\right]\right) \quad (24)$$

$$\text{ReLU}\left(G\left[(\mathbf{CL}_v^h)_{(p,q)}(F[\text{RoI}])\right]\right) = \max\left(0, G\left[(\mathbf{CL}_v^h)_{(p,q)}(C[\text{RoI}])\right]\right) \quad (25)$$

$$\text{ReLU}\left(G\left[(\mathbf{CL}_v^h)_{(p,q)}(F[\text{RoI}])\right]\right) = \max\left(0, G\left[(\mathbf{CL}_v^h)_{(p,q)}(I[\text{RoI}])\right]\right) \tag{26}$$

The advantage of employing ELU function permits to push mean unit activation closer to zero with lower computational complexity.

$$\text{fun}(G) = \begin{cases} G & \text{if } G > 0 \\ \alpha(e^G - 1) & \text{if } G \leq 0 \end{cases} \tag{27}$$

The output from the ELU layer, when fed with the feature map for convolution according to interval-valued is mathematically formulated as given below.

$$\text{CL}_v^h = \text{fun}(\text{CL}_v^{(h-1)}) \tag{28}$$

From the above equation (28), CL_v^h symbolizes the input, where $\text{CL}_v^{(h-1)}$ represents the output, with fun representing the activation function in the h layer. Finally, the brain patterns produced from the convolution and pooling layers are provided as input to the fully connected layers for starting the brain MRI image classification, with the objective of detecting distinct brain tumor classes. The output produced from the fully connected layers is mathematically stated as given below.

$$\begin{aligned} \text{PAC}_f^h = \sum_{p=1}^{\text{size}(FM)} \sum_{i=1}^{m} \sum_{j=1}^{n} \Bigg(& \text{BI}_{(f,p,i,j)}^h \cdot \text{CL}_v^{(h-1)}\left[T[\text{RoI}]\right], \\ & \text{CL}_v^{(h-1)}[F], \\ & \text{CL}_v^{(h-1)}\left[C[\text{RoI}]\right], \\ & \text{CL}_v^{(h-1)}\left[I[\text{RoI}]\right] \Bigg)_{(i,j)} \end{aligned} \tag{29}$$

From the above equation (29), $\text{BI}_{(f,p,i,j)}^h$ represents the weight associated with (i, j) in the p-th feature map of layer $h-1$ and the f-th unit in layer h respectively. The weights are tuned optimally using the proposed polynomial attention coefficient function. The best tumor detection results are discovered based on the fitness function as given below.

$$ff = \frac{1}{N}\sum_{i=1}^{N}(EO_i - PO_i)^2 \tag{30}$$

From the above equation (30), the fitness function ff results are arrived at based on the expected output EO_i and the predicted output PO_i for an overall of N samples. The flowchart of the Interval-valued Quadri-partitioned Neutrosophic Polynomial Attention-based Deep Convolutional Neural Network is demonstrated in Figure 4.

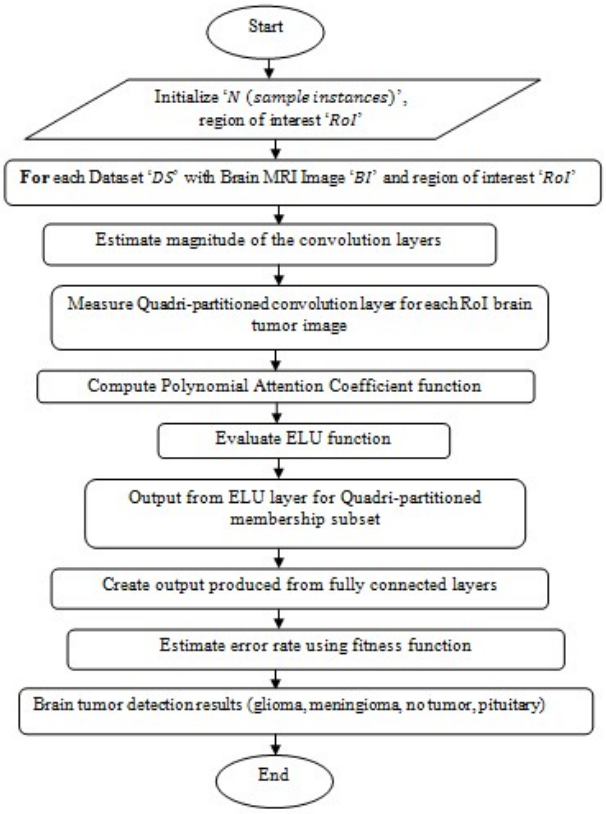

FIGURE 4. Flowchart of Interval-valued Quadri-partitioned Neutrosophic Polynomial Attention-based Deep Convolutional Neural Network.

The pseudo code representation of the Interval-valued Quadri-partitioned Neutrosophic Polynomial Attention-based Deep Convolutional Neural Network is given below.

As given in the below algorithm, Differential Quadri-partitioned Neutrosophic brain MRI RoI detected results are subjected to the classification process for detecting computationally efficient results. With this objective, the overall Deep CNN is split into convolution layers where with the aid of distinct magnitude the convoluted results are obtained via Interval-valued and Polynomial Attention Coefficient function for each Differential Quadri-partitioned Neutrosophic brain MRI RoI detected results. Next, the convoluted output is subjected to a pooling layer to minimize the feature map dimension via the ELU activation function according to different intervals. Finally, with the aid of output produced from the fully connected layers, efficient classification between four distinct classes (i.e., glioma, meningioma, no tumor, and pituitary) is made in a computationally efficient manner based on the fitness function

Input	Dataset 'DS', Brain MRI Image 'BI=$\{ BI_1, BI_2, \ldots, BI_N \}$'
Output	Computationally efficient brain tumor detection
Steps	
1	Initialize 'N (sample instances)', region of interest 'RoI'
2	Begin
3	For each Dataset 'DS' with Brain MRI Image 'BI' and region of interest 'RoI'
	// Convolutional layers
4	Obtain magnitude of the convolution layers as given in (16)
5	Obtain Quadri-partitioned convolution layer for each RoI brain tumor image as given in (17), (18), (19) and (20)
6	Evaluate Polynomial Attention Coefficient function as given in (21)
	// Pooling layer
7	Evaluate ELU function as given in (22)
8	Obtain output from the ELU layer for Quadri-partitioned membership subset as given in (23), (24), (25) and (26)
9	Obtain output from the ELU layer as given in (27) and (28)
	// Fully connected layers
10	Generate output produced from the fully connected layers as given in (29)
	// Error evaluation
11	Measure error rate using fitness function as given in (30)
12	Return detected results ('glioma', 'meningioma', 'no tumor', 'pituitary')
13	End for
14	End

Algorithm 1. Interval-valued Quadri-partitioned Neutrosophic Polynomial Attention-based Deep Convolutional Neural Network

4. **Experimental setup**

The proposed Differential Neutrosophic Polynomial Attention-based Deep Convolutional Neural Network (DNPA-DCNN) method is developed using MATLAB 2017. The Brain Tumor MRI dataset (https://www.kaggle.com/datasets/masoudnickparvar/brain-tumor-mri-dataset) used in Differential Neutrosophic Polynomial Attention-based Deep Convolutional Neural Network (DNPA-DCNN) is a combination of three datasets, fig share, SARTAJ and Br35H respectively. This Brain Tumor MRI dataset contains 7023 images on human brain MRI images was used in this study, 90% (6320) of which was employed as the training images and 10% (702) of which was employed as the testing images were split into four distinct classes, namely,

glioma, meningioma, no tumor and pituitary. To evaluate the proposed system, several performance measure metrics like, PSNR, specificity, brain tumor detection accuracy and brain tumor detection time are used that are computed with the help of equations (31) to (35).

5. **Comparative Study**

In this section, the proposed DNPA-DCNN method is compared with the existing methods such as [1], and [2] based on five certain metrics such as PSNR, specificity, brain tumor detection accuracy, brain tumor detection time, and sensitivity. The brain MRI images 50 to 500 are considered for experiments conduction. The performance results are presented through tabular data and graphical representations for comparison.

5.1. *Impact of PSNR*

PSNR associates to an MRI brain images immune function to noise external interference signals. When PSNR level is higher, the noisy interference signal's influence on the MRI brain image is minimum. The optimal PSNR value ranges between 40 and 60 dB. It is calculated by using the equation (31) as given below, where the value of 'MAX' is '255' and 'MSE' refers to the mean square error.

$$\text{PSNR} = 10 \log_{10} \left(\frac{\text{MAX}}{\text{MSE}} \right) \tag{31}$$

$$\text{MSE} = \frac{1}{MN} \sum_{i=1}^{M} \sum_{j=1}^{N} [\text{BI}(i,j) - \text{RI}(i,j)]^2 \tag{32}$$

From the above equations (31) and (32), the resultant PSNR is arrived at based on the cumulative square estimation error between the input brain image $\text{BI}(i,j)$ and the resultant image $\text{RI}(i,j)$ respectively.

In the first iteration, the PSNR calculations for the proposed DQNI-PADCNN method, existing methods, Deep learning [1], and CNN-based brain tumor classification [2] are detailed below.

Proposed DQNI-PADCNN PSNR Calculations The input brain image is 39.05 KB and the resultant image is 38.25 KB

MSE: $(39.05 - 38.25)^2 = (0.8)^2 = 0.64$

PSNR: $10 \log_{10} \left(\frac{255*255}{0.64}\right) = 10 \log_{10}(101601) = 50.69$ dB

Deep Learning [1] PSNR Calculations The input brain image is 39.05 KB and the resultant image is 38.15 KB

MSE: $(39.05 - 38.15)^2 = (0.9)^2 = 0.81$

PSNR: $10 \log_{10} \left(\frac{255*255}{0.81}\right) = 10 \log_{10}(80277) = 49.04$ dB

CNN-based Brain Tumor Classification [2] PSNR Calculations : The input brain image is 39.05 KB and the resultant image is 1.05 KB

MSE: $(39.05 - 38)^2 = (1.05)^2 = 1.1025$

PSNR: $10 \log_{10} \left(\frac{255*255}{1.1025}\right) = 10 \log_{10}(58979.59) = 47.70$ dB

According to the above calculations, similar results are provided for 10 different simulation runs performed with varying sizes and their results are provided in Table 1.

Table 1. Tabulations of PSNR using DQNI-PADCNN, deep learning [1] and CNN-based brain tumor classification [2]

Brain MRI Size	DQNI-PADCNN (dB)	Deep Learning (dB)	CNN-based (dB)
39.05	50.06	49.04	47.70
45.64	40.45	38.64	37.73
55.17	45.71	41.81	40.63
54.62	45.08	43.94	42.46
44.90	46.19	42.78	41.68
45.46	46.33	44.84	43.72
43.32	53.32	51.60	50.74
43.90	45.20	42.33	41.93
38.95	44.60	42.78	41.89
32.89	43.67	42.55	41.36

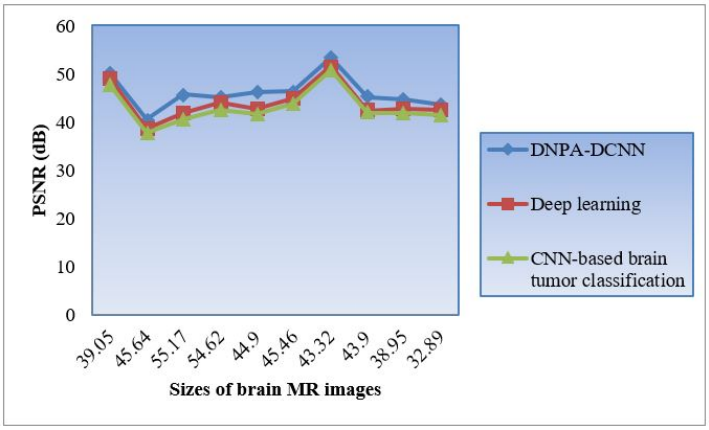

FIGURE 5. Performance analysis of PSNR versus different sizes of brain MR images.

Figure 5 given above illustrates the graphical representation of PSNR results of varying sizes for a simulation of 10 runs using the three methods, DQNI-PADCNN, deep learning [1], and CNN-based brain tumor classification respectively. Neither increasing nor decreasing trends are observed owing to the distinct sizes used for simulation. But comparative results showed betterment using DQNI-PADCNN than [1] and [2]. The reason behind the improvement was by applying the Differential Quadri-partitioned Neutrosophic function for Region of Interest detection, all the four measures, i.e., truth, false, contradiction, and ignorance membership results were obtained separately without affecting others (i.e., overlap results between truth and false, overlap results between false and ignorance results, overlap results between ignorance and contradiction results) in the decision-making process. In this way, the uncertainty involved during the region of interest detection was made in an efficient manner via differential quadri-partitioned entropy of the corresponding neutrosophic set. This in turn improved the Peak Signal-to-Noise-Ratio (PSNR) using DQNI-PADCNN by 5% compared to [1] and 7% compared to [2].

5.2. *Impact of Brain Tumor Detection Accuracy*

Brain tumor detection accuracy is defined as the ratio of the number of samples properly classified for disease detection. It is mathematically determined as given below.

$$\mathrm{BTD}_{\mathrm{acc}} = \sum_{i=1}^{N} \frac{S_{AD}}{S_i} \times 100 \tag{33}$$

From the above equation (33), brain tumor detection accuracy $\mathrm{BTD}_{\mathrm{acc}}$ is measured by taking into consideration the brain tumor samples S_i and the brain tumor samples accurately detected as S_{AD}. It is measured in terms of percentage (%). The performance analysis of

brain tumor detection accuracy is measured in the first iteration to validate the significance of the proposed DQNI-PADCNN and existing methods, Deep learning [1], and CNN-based brain tumor classification [2] as given below.

Proposed DQNI-PADCNN Brain Tumor Detection Accuracy The number of correctly identified brain tumor images is 48 and the total number of brain tumor images is 50. Thus, the brain tumor detection accuracy is measured as, $BTD_{acc}(DNPA-DCNN) = \frac{48}{50} \times 100 = 96\%$
Deep Learning [1] Brain Tumor Detection Accuracy The number of correctly identified brain tumor images is 46 and the total number of brain tumor images is 50. Thus, the brain tumor detection accuracy is measured as, $BTD_{acc}(DeepLearning) = \frac{46}{50} \times 100 = 92\%$
CNN-based Brain Tumor Classification [2] Brain Tumor Detection Accuracy The number of correctly identified brain tumor images is 45 and the total number of brain tumor images is 50. Thus, the brain tumor detection accuracy is measured as, $BTD_{acc}(CNN-basedBrainTumorClassification) = \frac{45}{50} \times 100 = 90\%$

Based on the above calculations by substituting the values in (33), similar results are performed for 10 different simulation runs with varying sizes and their results are listed in table 2.

TABLE 2. Tabulations of accuracies using DQNI-PADCNN, deep learning [1] and CNN-based brain tumor classification [2]

Brain MRI Size	DQNI-PADCNN (dB)	Deep Learning (dB)	CNN-based (dB)
50	96.00	92.00	90.00
100	95.35	89.25	85.35
150	93.10	88.65	84.10
200	92.25	86.45	83.25
250	90.45	85.35	80.10
300	89.75	84.25	78.25
350	88.45	82.35	77.10
400	87.65	79.10	76.45
450	86.10	78.35	76.10
500	85.25	76.65	74.10

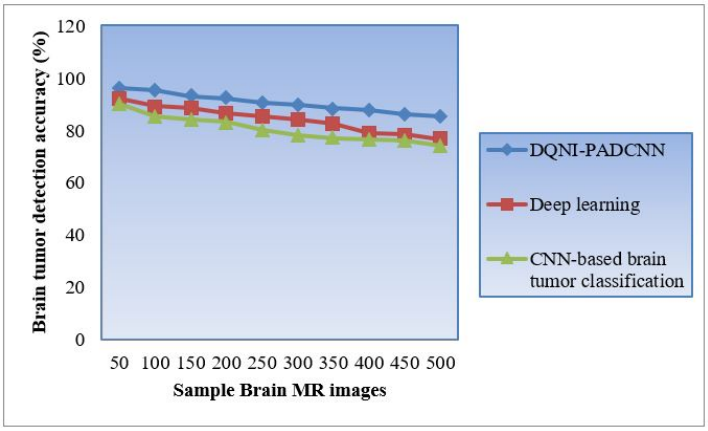

FIGURE 6. Performance analysis of accuracies versus different sample brain MR images.

Figure 6 gives the brain tumor detection accuracy comparison for all three methods. All three methods are trained for a total of 10 numbers of epochs. The accuracy shown here is specifically the validation accuracy i.e., the accuracy involved during the detection of brain tumor. For all the methods the brain tumor detection accuracy is high at the initial state of the training and towards the end of the training it gets to a value of 85.25% using DQNI-PADCNN, 76.55% using [1] and 74.10% using [2] respectively. It is entirely evident from the comparison graph that better performance is given by the proposed method with DQNI-PADCNN. The DQNI-PADCNN method has a better brain tumor detection accuracy curve and convergence rate than other methods [1] and [2]. The accuracy improvement DQNI-PADCNN

method owes to the application of an Interval-valued Quadri-partitioned Neutrosophic Polynomial Attention-based Deep Convolutional Neural Network. By applying this model, brain pattern extraction is made based on the adjoining convolution layers' results according to distinct intervals with the objective of detecting various classes of brain tumors. The adjoining convolution layers results were obtained using an Interval-valued Quadri-partitioned Neutrosophic Polynomial Attention Coefficient function that in turn only concentrated on a subset of target regions that in turn improved brain tumor samples accurately detected being higher. This in turn improved the brain tumor detection accuracy of the DQNI-PADCNN method by 7% compared to [1] and 13% compared to [2].

5.3. *Impact of Brain Tumor Detection Time*

Brain tumor detection time metric is estimated as the time used to detect the brain tumor and it is expressed as follows.

$$\mathrm{BTD}_{\mathrm{time}} = \sum_{i=1}^{N} S_i \cdot \mathrm{Time(ff)} \tag{34}$$

From the above equation (34), brain tumor detection time $\mathrm{BTD}_{\mathrm{time}}$ is measured by taking into account the brain samples MRI images S_i and the time consumed in returning the fitness function results that provide us with the actual time consumed in brain tumor detection $\mathrm{Time}(ff)$. It is measured in terms of milliseconds (ms).In the first iteration, the brain tumor detection time results are validated and listed in Table 3.

Proposed DQNI-PADCNN Brain Tumor Detection Time

The time taken for detecting one tumor affected image is 0.31ms and the number of brain tumor images is 50. Thus, the brain tumor detection time is estimated as,

$BTD_{time}(DNPA - DCNN) = 50 \times 0.31 = 15.5$ ms

Deep Learning[1] Brain Tumor Detection Time

The time taken for detecting one tumor affected image is 0.45ms and the number of brain tumor images is 50. Thus, the brain tumor detection time is estimated as,

$BTD_{time}(DeepLearning) = 50 \times 0.45 = 22.5$ ms

CNN-based Brain Tumor Classification[2] Brain Tumor Detection Time

The time taken for detecting one tumor affected image is 0.50ms and the number of brain tumor images is 50. Thus, the brain tumor detection time is estimated as,

$BTD_{time}(CNN - basedBrainTumorClassification) = 50 \times 0.50 = 25$ ms

Based on the above calculations by substituting the values in (34), similar results are performed for 10 different simulation runs with varying sizes and their results are listed in Table 3

TABLE 3. Tabulations of detection time using DQNI-PADCNN, deep learning [1] and CNN-based brain tumor classification [2]

Brain MRI Size	DQNI-PADCNN (dB)	Deep Learning (dB)	CNN-based (dB)
50	15.5	22.5	25
100	16.25	30.35	40.45
150	20.10	36.55	50.25
200	23.45	48.15	65.05
250	26.25	60.65	80.25
300	33.25	68.05	100.25
350	37.45	80.15	115.15
400	53.05	90.25	125.25
450	60.25	100.05	140.45
500	70.85	110.25	155.25

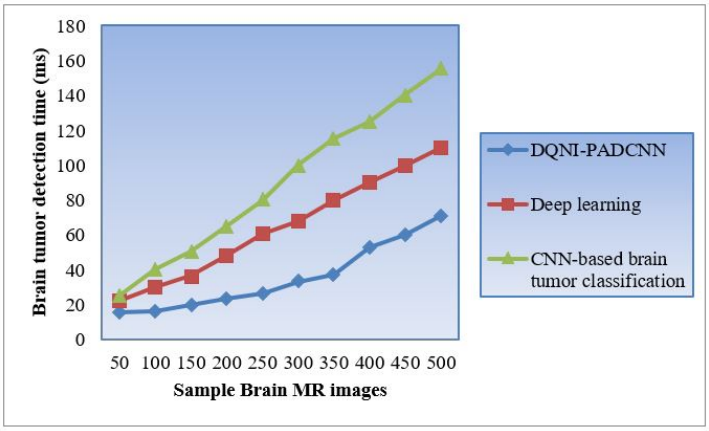

FIGURE 7. Performance analysis of specificity versus different sample brain MR images.

Now coming to Figure 7, we can see that the brain tumor detection time for all the methods has a low value at the start of epoch one and converges to 70.85ms using DQNI-PADCNN and 110.25ms using [1], 155.25ms using [2] respectively at the tenth epoch. Out of all the different methods our proposed DQNI-PADCNN has a better convergence rate. It converges to the minimum value among all the other methods. A very high value for brain tumor detection time loss is found for CNN-based brain tumor classification but it successfully converges towards the end. Deep learning also starts from a very high value and later it converges. However, our proposed DQNI-PADCNN method shows a steady performance throughout the training session. So, from the brain tumor detection time comparison plot, we can conclude that our proposed method has superior performance for the detection of the location of distinct tumors. The reason behind the minimization of time was due to the application of an Interval-valued Quadri-partitioned Neutrosophic Polynomial Attention-based Deep Convolutional Neural Network. By applying this algorithm, the overall process of brain tumor detection was split into convolution layers employing distinct magnitude via Quadri-partitioned Neutrosophic ReLU activation function the convoluted results were initially obtained. Next, by employing an interval-valued in addition to the polynomial attention coefficient to the ELU activation function the feature map dimension was reduced. Finally, the classification was made based on the fitness function that in turn reduced the brain tumor detection time using the DQNI-PADCNN method by 45% compared to [1] and 59% compared to [2].

5.4. *Impact of specificity*

Specificity refers to the probability of a test to correctly identify people without brain tumor disease. It is mathematically stated as given below

$$\text{Spe} = \frac{TN}{TN + FP} \tag{35}$$

From the above equation (35), the specificity rate 'Spe' is measured by taking the true negative values 'TN' (i.e., non-tumor patients correctly identified as patients with non-tumor) and the false positive values 'FP' (i.e., healthy people incorrectly identified as tumor patients) respectively. . The performance analysis of specificity is measured in the first iteration to validate the efficiency of the methods and detailed comparisons are made with [1] and [2] as given below.

Proposed DQNI-PADCNN Specificity
True negative value is 46 and False positive value is 4.
Then, the specificity is determined as,
$Spe(DNPA - DCNN) = \frac{46}{46+4} = 0.92$
Deep Learning [1] Specificity
True negative value is 45 and False positive value is 5.
Then, the specificity is determined as,
$Spe(DeepLearning) = \frac{45}{45+5} = 0.90$
CNN-based Brain Tumor Classification [2] Specificity
True negative value is 44 and False positive value is 6.
Then, the specificity is determined as,
$Spe(CNN - basedBrainTumorClassification) = \frac{44}{44+6} = 0.88$

TABLE 4. Tabulations of specificity using DQNI-PADCNN, deep learning [1] and CNN-based brain tumor classification [2]

Brain MRI Size	DQNI-PADCNN (dB)	Deep Learning (dB)	CNN-based (dB)
50	0.92	0.90	0.88
100	0.89	0.86	0.84
150	0.88	0.85	0.83
200	0.88	0.84	0.82
250	0.88	0.84	0.82
300	0.87	0.84	0.79
350	0.87	0.82	0.78
400	0.85	0.82	0.77
450	0.84	0.80	0.77
500	0.83	0.78	0.75

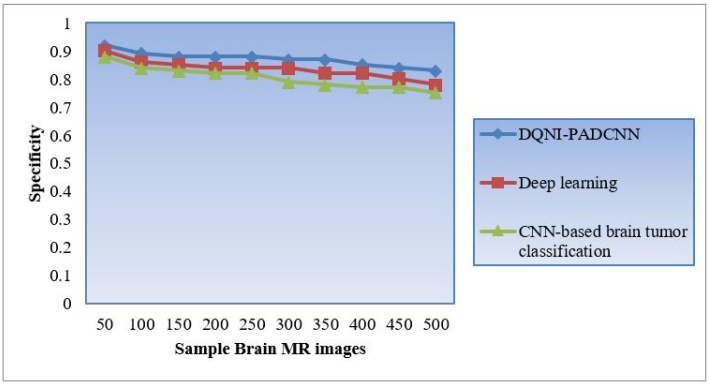

FIGURE 8. Performance analysis of specificity versus different sample brain MR images.

Figure 8 given above illustrates the specificity results of the three different methods. We utilize several colors to denote distinct methods, where blue color signifies the DQNI-PADCNN method specificity results, maroon and green denotes the [1] and [2] specificity results on the original sample brain MR images. From figure 8 it is seen that DQNI-PADCNN method achieves the best specificity results of brain tumors. Then, we amplify the tumor region via normalized Quadri-partitioned Neutrosophic function, aiming to provide a more comprehensive comparison. This in turn aid in achieving the best tumor detected results. These normalized results via Quadri-partitioned Neutrosophic function further indicate that maximum and minimum values from the gray brain test image focus on different tumor regions in recognizing correctly which help improving the performance of three tumor regions. This in turn improved the specificity using DQNI-PADCNN method by 4% compared to [1] and

8% compared to [2] respectively. Third, the performance analysis of brain tumor detection accuracy is measured to validate the significance of the proposed DQNI-PADCNN and existing methods, Deep learning [1] and CNN-based brain tumor classification [2].

5.5. *Impact of sensitivity*

Sensitivity is a performance metric and is also called recall. It is defined as the ratio of samples that are accurately classified to the overall relevant incidences. The sensitivity is mathematically computed as follows,

$$\text{Sensitivity} = \frac{TP}{TP + FN} \tag{36}$$

Where 'TP' denotes a True Positive, and 'FN' indicates a False Negative. The Sensitivity is determined in percentage (%). Finally, the sensitivity results are estimated and tabulated in Table 5 for the first iteration.

Proposed DQNI-PADCNN Sensitivity
The true positive value is 47 and the False negative value is 3.
Then, the sensitivity is determined as,
$Sensitivity(DNPA - DCNN) = \frac{47}{47+3} = 0.94$
Deep Learning [1] Sensitivity
True positive value is 46 and False negative value is 4.
Then, the sensitivity is determined as,
$Sensitivity(DeepLearning) = \frac{46}{46+4} = 0.92$
CNN-based Brain Tumor Classification [2] Sensitivity
True positive value is 44 and False negative value is 6.
Then, the sensitivity is determined as,
$Sensitivity(CNN - basedBrainTumorClassification) = \frac{44}{44+6} = 0.88$

Based on the above calculations by substituting the values in (36), similar results are given for 10 different simulation runs performed with varying sizes and their results are provided in Table 5.

TABLE 5. Tabulations of sensitivity using DQNI-PADCNN, deep learning [1] and CNN-based brain tumor classification [2]

Sample Brain MRI images	DQNI-PADCNN	Deep Learning	CNN-based
50	0.94	0.92	0.88
100	0.92	0.90	0.87
150	0.91	0.89	0.87
200	0.90	0.88	0.86
250	0.89	0.87	0.85
300	0.88	0.86	0.83
350	0.88	0.85	0.81
400	0.87	0.83	0.79
450	0.85	0.82	0.79
500	0.84	0.80	0.77

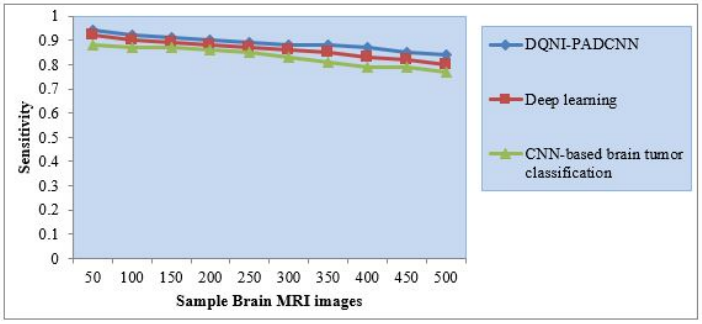

FIGURE 9. Performance analysis of sensitivity versus different sample brain MR images.

Figure 9 shows the results of sensitivity based on the sample brain MRI images. The performance of the sensitivity of the proposed DQNI-PADCNN method is compared with existing deep learning [1] and CNN-based brain tumor classification [2]. The x-axis denotes the number of brain MRI image samples and the y-axis indicates results of sensitivity using various methods. The above graphical illustrates that the proposed DQNI-PADCNN method attained higher sensitivity than the conventional methods. With the input of 50 brain MRI sample images, the overall sensitivity is measured as 94% in the DQNI-PADCNN method. Similarly, 92% and 88% of sensitivity is obtained in existing [1] and [2] respectively. From that, the sensitivity of the proposed DQNI-PADCNN method is found to be higher than the other methods. This is due to the application of Deep Convolutional Neural Networks for tumor detection. The designed classifier is employed to classify the images into four different classes. This helps to increase the sensitivity involved in tumor detection. Therefore, the

DQNI-PADCNN method enhances the sensitivity by 3% as compared to existing [1] and 7% as compared to existing [2] respectively.

6. Discussion

In this section, we compare the experimental results of the proposed DQNI-PADCNN with the ones of the existing methods, including the [1], the [2] based on various parameters, such as the PSNR, specificity, the brain tumor detection accuracy, the brain tumor detection time and the sensitivity. A comparison of the performance of the proposed method with the ones of the state-of-the-art methods is shown in Table 6.

TABLE 6. Comparison of proposed technique with state-of-the-art methods.

Metrics	DQNI-PADCNN	Deep Learning	CNN-based
PSNR (dB)	46.06	44.03	42.98
Specificity	0.87	0.83	0.80
Brain tumor detection accuracy (%)	90.43	84.24	80.48
Brain tumor detection time (ms)	112.64	107.50	127.32
Sensitivity	0.88	0.86	0.83

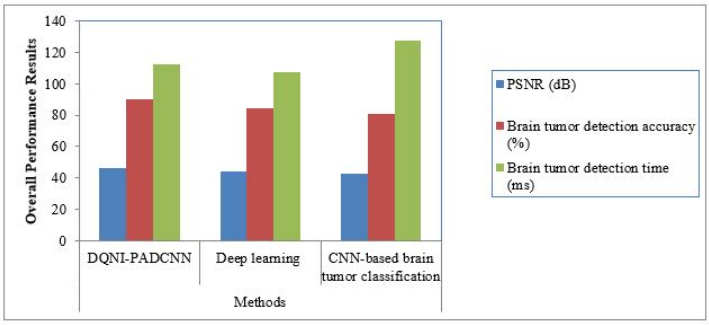

FIGURE 10. Comparison of different methods with respect to the PSNR, brain tumor detection accuracy,brain tumor detection time.

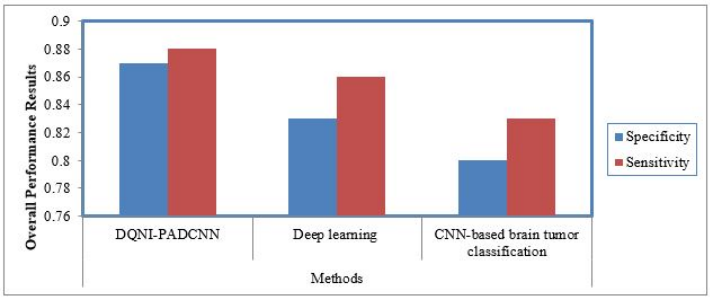

FIGURE 11. Comparison of different methods with respect to specificity and sensitivity.

Figure 10 and 11 compare the performances of different methods with respect to the PSNR, specificity, brain tumor detection accuracy, brain tumor detection time, and sensitivity. From the above table and graph, it can be seen that the proposed DQNI-PADCNN method outperforms Deep learning [1], the CNN-based brain tumor classification [2]. The overall observed performance results show that the accuracy is 90.43% using the DQNI-PADCNN method, 84.24% using [1], and 80.48% using [2]. The overall observed performance results show that the specificity is 0.87 using the DQNI-PADCNN method, 0.83 using [1], and 0.80 using [2]. The overall observed performance results show that the sensitivity is 0.88 using the DQNI-PADCNN method, 0.86 using [1], and 0.83 using [2]. The overall observed performance results show that the time is 112.64ms using the DQNI-PADCNN method, 107.50ms using [1], and 127.32ms using [2].

7. **Conclusion**

Proposed Differential Quadri-partitioned Neutrosophic Interval-valued Polynomial Attention-based Deep CNN (DQNI-PADCNN) is introduced for brain tumor detection using MR images. The designed method applies RoI detection and classification. Next, the Region of Interest detection is performed for each input brain MRI image using normalized Quadri-partitioned Neutrosophic function and differential entropy. In addition, the Interval-valued and Polynomial Attention Coefficient along with the ELU function are employed for the efficient detection of brain tumors. Experimental analysis is conducted to assess the performance of the DQNI-PADCNN method and compare it with conventional methods, using various metrics such as PSNR, accuracy, time, specificity, and sensitivity. The results of DQNI-PADCNN achieve higher PSNR, brain tumor detection accuracy, specificity, and sensitivity outperformed other conventional methods. Additionally, the DQNI-PADCNN method achieves a reduction in time compared to conventional methods. However, the dimensionality reduction was not performed in the proposed method to decrease the computational complexity involved in disease detection. In future work, novel machine learning methods will be comprised to address the dimensionality issue.

References

1. Praveen Kumar Ramtekkar, Anjana Pandey and Mahesh Kumar Pawar,Accurate detection of brain tumor using optimized feature selection based on deep learning techniques, Multimedia Tools and Applications, Springer (2023).
2. Yildiray Anagun,Smart brain tumor diagnosis system utilizing deep convolutional neural networks. Multimedia Tools and Applications, Springer (2023).
3. Javaria Amin, Muhammad Sharif, Anandakumar Haldorai, Mussarat Yasmin and Ramesh Sundar Nayak, Brain tumor detection and classification using machine learning: a comprehensive survey. Complex & Intelligent Systems, Springer 8 (2021) pp. 3161–3183.

4. Hasnain Ali Shah, Faisal Saeed, Sangseok Yun, Jun-Hyun Park, Anand Paul and Jae-Mo Kang, A Robust Approach for Brain Tumor Detection in Magnetic Resonance Images Using Finetuned Efficient Net. IEEE Access 10 (2022) pp. 65426 – 65438 10.1109/ACCESS.2022.3184113.
5. Md. Saikat Islam Khan, Anichur Rahman, Tanoy Debnath, Md. Razaul Karim, Mostofa Kamal Nasir, Shaha S. Band and Amir Mosavi, Iman Dehzang,Accurate brain tumor detection using deep convolutional neural network. Computational and Structural Biotechnology Journal, Elsevier .20 (2022) doi: 10.1016/j.csbj.2022.08.039.pp. 4733–4745.
6. Sakshi Ahuja, Bijaya Ketan Panigrahi and Tapan Kumar Gandhi, Enhanced performance of Dark-Nets for brain tumor classification and segmentation using colormap-based super pixel techniques. Machine Learning with Applications, Elsevier 7 (2022) https://doi.org/10.1016/j.mlwa.2021.100212.
7. Arkapravo Chattopadhyay and Mausumi Maitra,MRI-based brain tumor image detection using CNN based deep learning method. Neuroscience Informatics, Elsevier 2(4), (2022) pp. 2772-5286.
8. Agus Subhan Akbar, Chastine Fatichah andNanik Suciati, Single level UNet3D with multipath residual attention block for brain tumor segmentation. Journal of King Saud University – Computer and Information Sciences, Elsevier. 34(6)(2022)pp. 3247-3258.
9. Shubhangi Solanki, Uday Pratap Singh, Siddharth Singh Chouhan and Sanjeev Jain,Brain Tumor Detection and Classification Using Intelligence Techniques: An Overview. IEEE Access,11 (2023) Doi:10.1109/ACCESS.2023.3242666.pp. 12870 – 12886.
10. Omer Turk, Davut Ozhan,Emrullah Aca, Tahir Cetin Akinci and Musa Yilmaz, Automatic detection of brain tumors with the aid of ensemble deep learning architectures and class activation map indicators by employing magnetic resonance images. Journal of Medical Physics, (2022) Doi: 10.1016/j.zemedi.2022.11.010.
11. Abhishta Bhandari, Jarrad Koppen and Marc Agzarian, Convolutional neural networks for brain tumor segmentation. Insights into Imaging, Springer (2020) Doi:10.1186/s13244-020-00869-4.
12. Saeed Iqbal, Adnan N. Qureshi, Jianqiang Li and Tariq Mahmood, On the Analyses of Medical Images Using Traditional Machine Learning Techniques and Convolutional Neural Networks. Springer 30(5) (2023) ,.pp. 3173-3233. Doi: 10.1007/s11831-023-09899-9
13. Fatih Ozyurt, Eser Sert, Engin Avci and Esin Dogantekin¡ Brain Tumor Detection Based on Convolutional Neural Network with Neutrosophic Expert Maximum Fuzzy Sure Entropy. Measurement, Elsevier 147, (2019) https://doi.org/10.1016/j.measurement.2019.07.058.
14. Khan Muhammad, Salman Khan, Javier Del Ser and Victor Hugo C. de Albuquerque,Deep Learning for Multigrade Brain Tumor Classification in Smart Healthcare Systems: A Prospective Survey. IEEE Transactions on Neural Networks and Learning Systems 32(2), (2020) pp. 507 - 522 ,Doi: 10.1109/TNNLS.2020.2995800.
15. Amjad Rehman, Muhammad Attique Khan, Tanzila Saba, Zahid Mehmood, Usman Tariq and Noor Ayesha, Microscopic brain tumor detection and classification using 3D CNN and feature selection architecture. Wiley (2020) Doi: 10.1002/jemt.23597
16. Marcin Wozniak, Jakub Siłka and Michał Wieczorek,Deep neural network correlation learning mechanism for CT brain tumor detection. Neural Computing and Applications, Springer 35(2021)pp. 14611–14626 https://doi.org/10.1007/s00521-021-05841-x.
17. Emrah Irmak, Multi-Classification of Brain Tumor MRI Images Using Deep Convolutional Neural Network with Fully Optimized Framework. Iranian Journal of Science and Technology, Transactions of Electrical Engineering, Springer 45 (2021) pp. 1015–1036 https://doi.org/10.1007/s40998-021-00426-9.
18. A.Ghanbari Talouki., A.Koochari, S.A.Edalatpanah, Applications of Neutrosophic Logic in Image Processing: A Survey. Journal of Electrical and Computer Engineering Innovations 10(1) (2021) pp. 243-258 Doi: 10.22061/JECEI.2021.8069.474.

19. Sepideh Molaei, Niloofar Ghorbani, Fatemeh Dashtiahangar, Mohammad Peivandi, Yaghoub Pourasad and Mona Esmaeili,FDCNet: Presentation of the Fuzzy CNN and Fractal Feature Extraction for Detection and Classification of Tumors. Computational Intelligence and Neuroscience, Hindawi, (2022) https://doi.org/10.1155/2022/7543429.
20. Panimalar,,K. Mohana,,R. Parvathi, and S. Santhosh Kumar, Mathematical Morphological Operations for Quadri-Partitioned Neutrsophic Set, International Journal of Neutrosophic Science,23(2),(2023). https://doi.org/10.54216/IJNS.230207.
21. A. Panimalar , D. Aarthi and S. Santhosh Kumar, Medical Image Classification Using RNN in Quadri-Partitioned Neutrosophic Set, TuijinJishu/Journal of Propulsion Technology, 44 (4), (2023). https://doi.org/10.52783/tjjpt.v44.i4.1395.
22. R. Narmadhagnanam & A. Edward Samuel. Application of Secant Span in Medical Diagnosis. Neutrosophic Systems With Applications, 18 (2024) pp. 40-45. https://doi.org/10.61356/j.nswa.2024.18254.
23. Mahmoud Y. Shams., Romany M. Farag, Dalia A. Aldawody, Huda E. Khalid, Ahmed K. Essa, Hazem M. El-Bakry & A. A. Salama, Unveiling Similarities in the Code of Life: A Detailed Exploration of DNA Sequence Matching Algorithm. Neutrosophic Systems With Applications, 22 (2024) pp.13-30. https://doi.org/10.61356/j.nswa.2024.22369
24. A. Panimalar,D. Aarthi, S. Santhosh Kumar and Alapati Varalakshmi, Analysing Medical Image with Discrete Wavelet Transform Under Uncertainty, Int. J. Appl. Comput. Math ,9 (114) (2023). https://link.springer.com/article/10.1007/s40819-023-01566-8.
25. Traitement Vasileios Papageorgiou, Brain Tumor Detection Based on Features Extracted and Classified Using a Low Complexity Neural Network Traitement du Signal 38(3),(2021) pp. 547-554 Doi: https://doi.org/10.18280/ts.380302.
26. Carlos Granados,Quadripartitioned Single-Valued Neutrosophic Properties and Their Application to Factors Affecting Energy Prices. Process Integration and Optimization for Sustainability, Springer 7(3) (2023),pp. 575–582 Doi:10.1007/s41660-023-00310-5.
27. Rehan Ahmad Khan Sherwani,Tooba Arshad,Mohammed Albassam,Muhammad Aslam and Shumaila Abbas ,Neutrosophic entropy measures for the Weibull distribution: theory and applications. Complex & Intelligent Systems, Springer 7 (2021) pp. 3067–3076 https://doi.org/10.1007/s40747-021-00501-y.
28. Soheila Saeedi, Sorayya Rezayi, Hamidreza Keshavarz and R.Sharareh Niakan Kalhori, MRI-based brain tumor detection using convolutional deep learning methods and chosen machine learning techniques. BMC Medical Informatics and Decision Making 23(16), (2023) https://doi.org/10.1186/s12911-023-02114-6.

Received: Nov. 29, 2024. Accepted: May 19, 2025